

Publisher: GSA  
Journal: GEOL: Geology  
Article ID: G32136

1 **Dynamic constraints on the crustal-scale rheology of the Zagros**  
2 **fold belt, Iran**

3 **Philippe Yamato<sup>1,2\*</sup>, Boris J.P. Kaus<sup>2,3</sup>, Frédéric Mouthereau<sup>4</sup>, and Sébastien Castelltort<sup>2</sup>**

4 <sup>1</sup>*Geosciences Rennes, UMR CNRS 6118, Université de Rennes 1, F-35042 Rennes Cedex,*  
5 *France*

6 <sup>2</sup>*Department of Earth Sciences, E.T.H. Zürich, Sonneggstrasse 5, 8092 Zürich, Switzerland*

7 <sup>3</sup>*Department of Earth Sciences, University of Southern California, Los Angeles, USA*

8 <sup>4</sup>*UPMC Univ. Paris 06, UMR CNRS 7193, IStEP, 75252 Paris Cedex 5, France*

9  
10 \*E-mail: philippe.yamato@univ-rennes1.fr

11 **ABSTRACT**

12 Thin-skinned fold-and-thrust belts are generally considered as the result of contractional  
13 deformation of a sedimentary succession over a weak décollement layer. The resulting surface  
14 expression frequently consists of anti- and synclines, spaced in a fairly regular manner. It is thus  
15 tempting to use this spacing along with other geological constraints to obtain insights in the  
16 dynamics and rheology of the crust on geological time scales. Here we use the Zagros Mountains  
17 of Iran as a case study as it is one of the most spectacular, well-studied thin-skinned fold-and-  
18 thrust belts in the world. Both analytical and numerical models are employed to study what  
19 controls fold-spacing and under which conditions folding dominates over thrusting. The models  
20 show that if only a single basal décollement layer is present underneath a brittle sedimentary  
21 cover, deformation is dominated by thrusting which is inconsistent with the data of Zagros Fold  
22 Belt. If we instead take into account additional décollement layers that have been documented in

23 the field, a switch in deformation mode occurs and crustal-scale folding is obtained with the  
24 correct spacing and timescales. We show that fold spacing can be used to constrain the friction  
25 angle of the crust, which is  $\sim 5$  degrees in Zagros Fold Belt. This implies that on geological  
26 timescales, the upper crust is significantly weaker than previously thought, possibly due to the  
27 effect of fluids.

## 28 INTRODUCTION

29 It is often assumed that fold belts can be explained by folding of a sedimentary layer  
30 above a basal detachment formed by a weak layer. As the spacing between folds in such belts is  
31 quite regular, we can consider them as a large-scale natural experiment of crustal deformation.  
32 Ideally, it should be possible to combine fold spacing with other geological data and theory to  
33 constrain parameters such as crustal rheology that are difficult or impossible to constrain from  
34 field observations alone.

35 The classical explanation of folds in fold belts is that they are due to a folding instability,  
36 which is well known for a homogeneous sedimentary sequence with either a power-law viscous  
37 or an elastic rheology (Schmalholz et al., 2002; Burg et al., 2004; Schmalholz, 2006). The  
38 dominant wavelength  $\lambda_{dom}$ , for a viscous power-law layer of viscosity  $\eta_{sed}$  and with exponent  $n$   
39 overlying a linear viscous layer of viscosity  $\eta_{salt}$ , is given by (Schmalholz et al., 2002):

$$40 \quad \lambda_{dom} = 3.1 \left( \frac{\eta_{sed}}{n\eta_{salt}} \right)^{\frac{1}{6}} \sqrt{\frac{H_{salt}}{H_{sed}}} H_{sed} \quad (1)$$

41 where  $H_{sed}$  and  $H_{salt}$  are the thicknesses of the sedimentary cover and of the salt, respectively.  
42 The growth rate ( $q_{dom}$ ) of this instability non-dimensionalized over the background strain rate  
43  $\dot{\epsilon}$  is given by (Schmalholz et al., 2002):

$$44 \quad \frac{q_{dom}}{\dot{\epsilon}} = 2.5n \left( \frac{\eta}{n\eta_{salt}} \right)^{\frac{1}{3}} \frac{H_{salt}}{H_{sed}} = 2.5n \left( \frac{\lambda_{dom}}{3.1H_{sed}} \right)^2 \quad (2)$$

45 and a combination of numerical and analytical studies have shown that  $q_{dom}/\dot{\epsilon}$  should be larger  
46 than  $\sim 20$  for folding to form observable folds, rather than homogeneous thickening (e.g., Kaus  
47 et. al, 2008).

48 The Zagros Fold Belt of Iran constitutes a classical example of such a folded belt that is  
49 geologically (e.g., Stocklin, 1968; Alavi, 2004; McQuarrie, 2004; Sherkati and Letouzey, 2004;  
50 Mouthereau et al., 2007) and geophysically (e.g., Jahani et al., 2009; Hatzfeld and Molnar, 2010;  
51 Nissen et al., 2010) well studied due to excellent exposure and extensive seismic and borehole  
52 data from exploration. The main tectonic and stratigraphic units are summarized on Figure 1 and  
53 show that a particular feature of the Zagros Fold Belt is a consistent spacing of folds with a  
54 wavelength ( $\lambda_{dom}$ ) of  $14 \pm 3$  km. These folds are generally explained as detachment folding of  
55 the post-Cambrian sedimentary sequence above a basal weak layer constituted by the Hormuz  
56 salt.

57 The centroid depths of waveform-modeled earthquakes indicate that faulting is restricted  
58 to two structural levels located in the competent sediment cover units at 5–6 km depth and within  
59 the Precambrian basement at depth larger than 11 km down to depths of 30 km (e.g., Talebian  
60 and Jackson, 2004; Nissen et al., 2010). Seismic reflection profiles (Jahani et al., 2009) and field  
61 observations in the Fars region (Mouthereau et al., 2007) show a lack of major thrust faults  
62 cutting the folded cover up to the surface. This confirms that detachment folding rather than  
63 thrusting is the dominant deformation mode in the Zagros Fold Belt. In this aspect, the Zagros  
64 Mountains differ from other fold-and-thrust belts such as the Jura Mountains, where large-offset

65 faults are continuous across the stratigraphic sequence, well imaged through seismic studies  
66 (Simpson, 2009).

67 Detachment folding theory should thus be perfectly applicable to the Zagros Fold Belt.  
68 Equations (1) and (2) show that fold spacing depends strongly on the rheology of the overburden  
69 and on the thickness of the basal salt layer. In the Zagros, a linear viscous overburden ( $n = 1$ ) and  
70 a viscosity contrast of 100 between salt and overburden, requires a salt layer thickness of  $\sim 7.8$   
71 km to fit the observed spacing of folds (Equation 1). Yet, seismic data indicates that the  
72 thickness of the Hormuz salt is no more than 1 or 2 km (Jackson et al., 1990; Mouthereau et al.,  
73 2006; Jahani et al., 2009). If the sedimentary cover has a power law rheology instead, its power  
74 law exponent should be  $n \sim 23$  (Equation 2) to explain the data, which is considerably larger than  
75 estimates from rock creep experiments (Ranalli, 1995). Large power law exponents are often  
76 taken as evidence for a brittle rheology. Currently, however, there is no theory that can reliably  
77 predict the spacing of detachment folds in the case of a brittle overburden.

78 There is thus presently no satisfactory explanation for (1) why deformation in the Zagros  
79 Fold Belt is dominated by folding and not by thrusting and for (2) what controls the spacing of  
80 folds and how it is linked to crustal rheology. In order to address this, we performed thermo-  
81 mechanical numerical simulations to study the dynamics of detachment folding in the presence  
82 of a brittle sedimentary cover.

### 83 **NUMERICAL MODEL**

84 To study the effect of using visco-elasto-plastic rheologies on crustal dynamics, we have  
85 performed a series of numerical experiments using the finite element code MILAMIN\_VEP  
86 (e.g., Kaus, 2010 and GSA Data Repository DR1). The viscosities of the weak layers are  
87 assumed to be linear and constant, which is a reasonable approximation for the rheology of salt.

88 The brittle layers have a temperature-dependent rheology of limestone (see DR1), which  
89 correspond to the majority of rocks within the sedimentary cover (Fig. 1C, Mouthereau et al.,  
90 2007). A linear geotherm of  $25\text{ }^{\circ}\text{C.km}^{-1}$  is initially applied (see DR1). For the low-temperature  
91 conditions of the Zagros Fold Belt, stresses are such that the rocks effectively deform in the  
92 brittle regime. Our model domain is initially  $200 \times 7.225$  km in size (see DR1). The top boundary  
93 is a free surface with no erosion (see DR1) and a constant background strain rate of  $10^{-15}\text{ s}^{-1}$  is  
94 applied at the right of the model box, which results in 15% shortening after 5.5 Myrs consistent  
95 with geological constraints (see DR1). All other sides of the model have free slip conditions.  
96 Finally, to initiate the folding, the interface between the salt and the overburden rocks has  
97 random noise with maximum amplitude of 100 m. Model simulations are performed for 5.5  
98 Myrs, after which results are interpreted.

## 99 **RESULTS FROM NUMERICAL SIMULATIONS**

100 With a 1.5 km-thick single basal detachment layer underlying a homogeneous brittle  
101 sedimentary cover, the models develop faults rather than folds (Fig. 2B). Such faults develop at  
102 early stages with a spacing that is approximately twice the brittle layer thickness. Subsequent  
103 deformation is locked around these folds that have a box-fold geometry. Compared to the Zagros  
104 Fold Belt, we thus obtain a too large wavelength and an incorrect deformation style. Additional  
105 simulations where we varied the frictional parameters of the crust, or the viscosity of the salt  
106 layer gave similar results (see Fig. DR1). We thus infer that it is impossible to reproduce the  
107 observed finite wavelength of Zagros Fold Belt folds (Fig. 1) by considering only one weak basal  
108 décollement layer, unless this layer has an unrealistically large thickness.

109 A detailed look at the stratigraphic column, however, reveals that the sedimentary cover  
110 is not rheologically homogeneous. Instead there are several layers that are composed of relatively

111 weak rocks such as evaporites or shales (Fig. 1B, C, see detailed descriptions in McQuarrie,  
112 2004; Sherkati et al., 2006 and Mouthereau et al., 2007). A second set of simulations took this  
113 fine-scale rheological structure into account (Fig. 3). The results are remarkably different from  
114 the previous experiments: rather than being fault-dominated, deformation is now achieved by  
115 folding, with a final wavelength similar to the one observed in the Zagros Fold Belt (Fig. 3). An  
116 analysis of the simulation shows that the spacing of the folds is fixed at a very early stage, after  
117 which the individual structures grow without clear geometric pattern, in accordance with field  
118 constraints (Mouthereau et al., 2007). The initial fine-scale rheological stratification of the  
119 sediment cover of the Zagros Fold Belt thus has a first-order effect on the development of upper  
120 crustal-scale structures. These results are in full agreement with a recent study of active  
121 seismicity in the Zagros Fold Belt which showed that both the Hormuz salt layer and the  
122 intermediate layers are mechanically-weak zones that form barriers to rupture for active faults  
123 (Nissen et al., 2010).

#### 124 **CONSTRAINTS ON CRUSTAL RHEOLOGY**

125 The simulations presented in this study highlight the different modes of deformation that  
126 might occur in fold-and-thrust belts. However, they give limited insights into the underlying  
127 physics, as it remains unclear how sensitive the spacing of structures is to the rheology of the  
128 crust. For this reason, we developed a semi-analytical methodology drastically reducing the  
129 computational requirements that allows us to predict the outcome of numerical simulations in a  
130 large parameter space (see details in DR2). The resulting wavelength versus growth rate  
131 diagrams have a single maximum as a function of non-dimensional wavelength (Fig. 4A).  
132 Rigorously, these semi-analytical results are only valid for very small deformations. Yet, a  
133 comparison with numerical simulations reveals that they correctly predict the spacing of folds

134 even after 5.5 Myrs, which confirms that fold-spacing is selected at a very early stage in the  
135 evolution of a fold and thrust belt (Fig. 4A).

136 Results for a homogeneous and brittle sedimentary cover reveal that the dominant growth  
137 rate is smaller than 20, which essentially means that folding will not be able to overcome  
138 background pure-shear thickening. Indeed, our numerical simulations indicate that this leads to  
139 fault-dominated deformation rather than folding (box folds, Fig. 2). If, on the other hand, weak  
140 layers are taken into account in the sedimentary sequence, the growth rate is significantly larger  
141 and the dominant wavelength is reduced (Fig. 4B). The addition of a single weak layer is  
142 sufficient to switch deformation styles from fault- to fold- dominated, and elasticity has a minor  
143 effect only.

144 Using the same semi-analytical methodology, we performed a large number of  
145 simulations and found that the two most important parameters are the viscosity of the salt/weak  
146 layers and the friction angle of the crust, whereas rock density plays little to no role. Plots of  
147 dominant wavelength and growth rate versus those two parameters show an approximate equal  
148 dependence on the two parameters (Fig. 4). The results also show that weak layers in all cases  
149 yields growth rates that are sufficiently large for the folding instability to dominate faulting.

150 In the case of Zagros Fold Belt, the effective viscosity of salt has been determined to be  
151 close to  $10^{18}$  Pa.s, a value consistent with scaled laboratory-derived values (Spiers et al., 1990)  
152 and other modeling studies (Van Keken et al., 1993; Mouthereau et al., 2006). If we combine this  
153 with our method, we estimate that the effective friction angle for the crust in the Zagros Fold  
154 Belt on geological timescales is around  $5^{\circ} \pm 5^{\circ}$  (Fig. 4B).

## 155 **DISCUSSIONS AND CONCLUSIONS**

156 Contrary to the common view of fold belts that often consider a single major basal  
157 décollement only, we demonstrate through the example of the Zagros Mountains that the whole  
158 stratigraphic sequence might influence the dynamics of the belt. Heterogeneities within the  
159 sedimentary cover, and weak layers in particular, control whether deformation is dominated by  
160 crustal-scale folds or by thrusts. The stratigraphy of a fold belt plays a much larger role than  
161 previously appreciated and should thus be taken into account if one wishes to reconcile field  
162 observations with physically consistent models of geological processes.

163 Balancing geological cross-sections in fold-thrust belts is a difficult exercise that aims at  
164 providing a consistent structural and kinematic interpretation of usually independent structural  
165 data. Our method paves the way for developing future generations of 2D and 3D dynamic  
166 reconstruction models for fold and thrust belts (e.g., Lechmann et al. 2010).

167 Moreover, we show that the regular spacing of folds puts constraints on the rheology of  
168 the crust on geological timescales. In the case of Zagros Fold Belt, the value for the friction  
169 angle we obtained in this manner is small ( $<10^\circ$ ), which indicates that the crust was rather weak,  
170 potentially due to large fluid pressures (e.g., Huismans et al. 2005).

## 171 **ACKNOWLEDGMENTS**

172 This work benefits from fruitful discussions with L. Le Pourhiet, S. Schmalholz and  
173 Y. Podladchikov. Constructive reviews from D. van Hinsbergen and 2 anonymous reviewers  
174 have also largely contributed to improve the manuscript. BJP Kaus was partly supported by  
175 ERC Starting Grant 258830.

## 176 **REFERENCES CITED**

177 Alavi, M., 2004, Regional stratigraphy of the Zagros fold-thrust belt of Iran and its proforeland  
178 evolution: American Journal of Science, v. 304, p. 1–20, doi:10.2475/ajs.304.1.1.

- 179 Burg, J.-P., Kaus, B.J.P., and Podladchikov, Y.Y., 2004, Dome structures in collision orogens:  
180 Mechanical investigation of the gravity/compression interplay, *in* Whitney, D.L., et al., eds.,  
181 Gneiss Domes in Orogeny: Geological Society of America Special Paper 380, p. 47–66.
- 182 Hatzfeld, D., and Molnar, P., 2010, Comparisons of the kinematics and deep structures of the  
183 Zagros and Himalaya and of the Iranian and Tibetan plateaus and geodynamic implications:  
184 Review of Geophysics, v. 48, no. RG2005, doi:10.1029/2009RG000304.
- 185 Huismans, R. S., S. J. H. Buiter, and C. Beaumont (2005), Effect of plastic-viscous layering and  
186 strain softening on mode selection during lithospheric extension, *J. Geophys. Res.*, 110, B02406,  
187 doi:10.1029/2004JB003114.
- 188 Jackson, M.P.A., Cornelius, R.R., Craig, C.H., Gansser, A., Stöcklin, J., and Talbot, C.J., 1990,  
189 Salt diapirs of the Great Kavir, central Iran: Geological Society of America Memoir 177,  
190 139 p.
- 191 Jahani, S., Callot, J.P., Letouzey, J., and Frizon de Lamotte, D., 2009, The eastern termination of  
192 the Zagros Fold-and-Thrust Belt, Iran: Structures, evolution, and relationships between salt  
193 plugs, folding, and faulting: *Tectonics*, v. 28, p. TC6004, doi:10.1029/2008TC002418.
- 194 Kaus, B.J.P., 2010, Factors that control the angle of shear bands in geodynamic numerical  
195 models of brittle deformation: *Tectonophysics*, v. 484, p. 36–47,  
196 doi:10.1016/j.tecto.2009.08.042.
- 197 Kaus, B.J.P., Steedman, C., and Becker, T.W., 2008, From passive continental margin to  
198 mountain belt: Insights from analytical and numerical models and application to Taiwan:  
199 *Physics of the Earth and Planetary Interiors*, v. 171, p. 235–251,  
200 doi:10.1016/j.pepi.2008.06.015.

- 201 Lechmann, S.M., Schmalholz, S.M., Burg, J.-P., Marques, F.O., 2010. Dynamic unfolding of  
202 multilayers: 2D numerical approach and application to turbidites in SW Portugal.  
203 *Tectonophysics* 494 (1-2), p. 64-74.
- 204 McQuarrie, N., 2004, Crustal scale geometry of the Zagros fold-thrust belt, Iran: *Journal of*  
205 *Structural Geology*, v. 26, p. 519–535, doi:10.1016/j.jsg.2003.08.009.
- 206 Mouthereau, F., Lacombe, O., and Meyer, B., 2006, The Zagros folded belt (Fars Iran):  
207 Constraints from topography and critical wedge modelling: *Geophysical Journal*  
208 *International*, v. 165, p. 336–356, doi:10.1111/j.1365-246X.2006.02855.x.
- 209 Mouthereau, F., Tensi, J., Bellahsen, N., Lacombe, O., De Boisgrollier, T., and Kargar, S., 2007,  
210 Tertiary sequence of deformation in a thin-skinned/thick skinned collision belt: The Zagros  
211 Folded Belt (Fars, Iran): *Tectonics*, v. 26, p. TC5006, doi:10.1029/2007TC002098.
- 212 Nissen, E., Yamini-Fard, F., Tatar, M., Gholamzadeh, A., Bergman, E., Elliott, J.R., Jackson,  
213 J.A., and Parsons, B., 2010, The vertical separation of mainshock rupture and  
214 microseismicity at Qeshm island in the Zagros fold-and-thrust belt, Iran: *Earth and Planetary*  
215 *Science Letters*, v. 296, p. 181–194, doi:10.1016/j.epsl.2010.04.049.
- 216 Ranalli, G., 1995, *Rheology of the Earth*, 2<sup>nd</sup> ed.: London, Chapman and Hall.
- 217 Schmalholz, S.M., 2006, Scaled amplification equation: A key to the folding history of buckled  
218 viscous single-layers: *Tectonophysics*, v. 419, p. 41–53, doi:10.1016/j.tecto.2006.03.008.
- 219 Schmalholz, S.M., Podladchikov, Y., and Burg, J.-P., 2002, Control of folding by gravity and  
220 matrix thickness: Implications for large-scale folding: *Journal of Geophysical Research*,  
221 v. 107, 2005, doi:10.1029/2001JB000355.

- 222 Sherkati, S., and Letouzey, J., 2004, Variation of structural style and basin evolution in the  
223 central Zagros (Izeh zone and Dezful embayment): Iran: *Marine and Petroleum Geology*,  
224 v. 21, p. 535–554, doi:10.1016/j.marpetgeo.2004.01.007.
- 225 Sherkati, S., Letouzey, J., and Frizon de Lamotte, D., 2006, Central Zagros fold-thrust belt  
226 (Iran): New insights from seismic data, field observation, and sandbox modelling: *Tectonics*,  
227 v. 25, p. TC4007, doi:10.1029/2004TC001766.
- 228 Simpson, G.D.H., 2009, Mechanical modeling of folding versus faulting in brittle-ductile  
229 wedges: *Journal of Structural Geology*, v. 31, p. 369–381, doi:10.1016/j.jsg.2009.01.011.
- 230 Spiers, C.J., Schutjens, P.M.T.M., Brzesowsky, R.H., Peach, C.J., Liezenberg, J.L., and Zwart,  
231 H.J., 1990, Experimental determination of constitutive parameters governing creep of  
232 rocksalt by pressure solution: *Geological Society of London Special Publication 54*, p. 215–  
233 227.
- 234 Stocklin, J., 1968, Structural history and tectonics of Iran; A review: *The American Association*  
235 *of Petroleum Geologists Bulletin*, v. 52, p. 1229–1258.
- 236 Talebian, M., and Jackson, J.A., 2004, Reappraisal of earthquake focal mechanisms and active  
237 shortening in the Zagros mountains of Iran: *Geophysical Journal International*, v. 156,  
238 p. 506–526, doi:10.1111/j.1365-246X.2004.02092.x.
- 239 Van Keken, P.E., Spiers, C.J., Van den Berg, A.P., and Muyzert, E.J., 1993, The effective  
240 viscosity of rocksalt: Implementation of steady state creep laws in numerical models of salt  
241 diapirism: *Tectonophysics*, v. 225, p. 457–476, doi:10.1016/0040-1951(93)90310-G.

## 242 **FIGURE CAPTIONS**

243 Figure 1. Field constraints for the Zagros folded belt. A: Topography illustrates the regular  
244 spacing of folds with amplitude ~500–1000 m over on an area of ~80 000 km<sup>2</sup>. Fold crest length

245 are of ~50 km in average. Inset shows the distribution of fold wavelengths measured for 88  
246 anticlines from the Zagros Folded Belt. B: Cross-section (aa') across the Zagros Fold Belt based  
247 on field measurement (Mouthereau et al., 2007).  $\lambda$  corresponds to the average wavelength of the  
248 folds. This value is slightly smaller than the 15.8 +/- 5.3 km from Mouthereau et al. (2007) that  
249 took into account the folds from the whole Fars area. MFF and SF correspond to the seismogenic  
250 Mountain Front Fault and the Surmeh Fault, respectively, associated with basement faulting.  
251 Vertical fold velocity is 0.3–0.6 mm.yr<sup>-1</sup>. C: Synthetic stratigraphic log where WL1, WL2 and  
252 WL3 correspond to the weak layers in the sedimentary sequence (Fm: Formation).

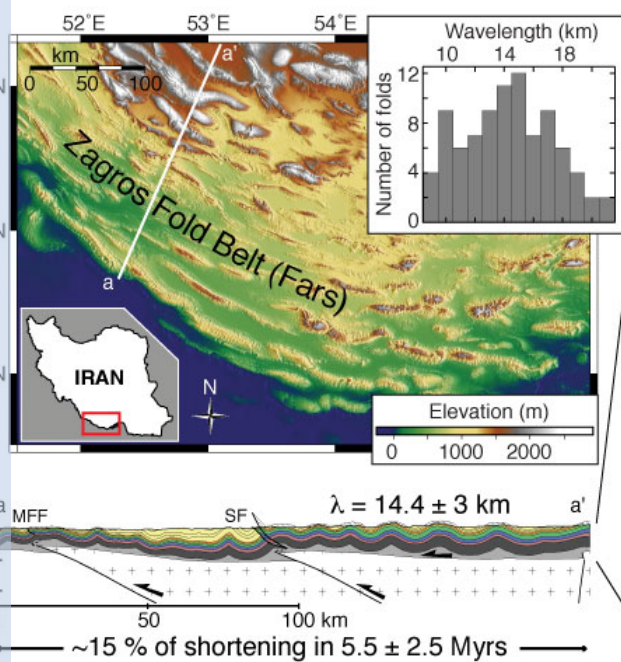
253 Figure 2. Simulation with a basal décollement layer only. A: Initial setup with a sedimentary  
254 thickness of 7.225 km. All rocks above the basal salt layer are homogeneous and have a friction  
255 angle of 5° and a cohesion of 20 MPa. A background strain rate of 10<sup>-15</sup> s<sup>-1</sup> is imposed at the  
256 right model boundary. B: Geometry, strain rate, and vertical velocities after 1.5 Myrs and 5.5  
257 Myrs respectively. Deformation is localized along crustal-scale plastic shear zones and  
258 deformation structures are fault-dominated.

259 Figure 3. Simulation with intermediate crustal detachment layers. A: Initial setup as in figure 2,  
260 but with three additional weak crustal detachment layers with 10<sup>18</sup> Pa.s. B: Snapshots of  
261 geometry, strain rate and vertical velocities at different times, which illustrate that crustal-scale  
262 folds rather than faults dominate the deformation pattern. Note that folds do not grow  
263 continuously with time, but rather grow to certain amplitude after which activity switches to a  
264 different fold.

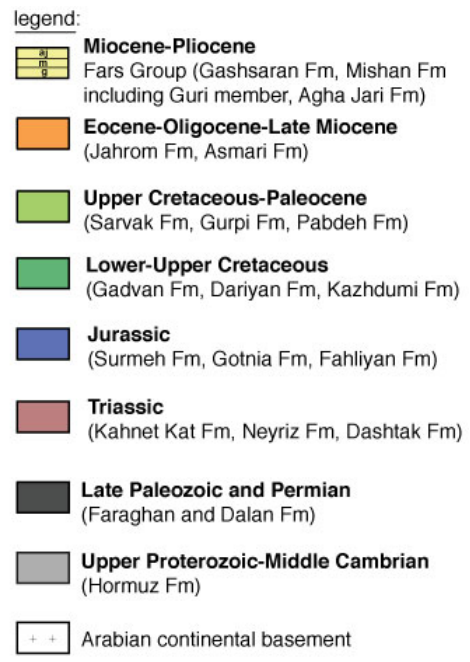
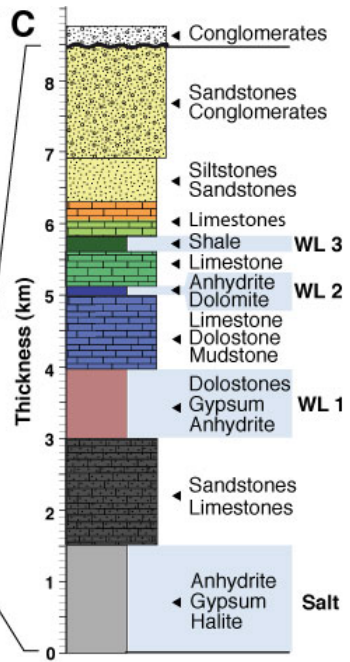
265 Figure 4. Influence of multiple weak layers and elasticity on folding.  $\lambda$ , H, q and  $\dot{\epsilon}$  corresponds  
266 to the wavelength, the total thickness, the growth rate and the background strain rate,  
267 respectively. VP and VEP correspond to visco-plastic and visco-elasto-plastic simulations,

268 respectively. This diagram was produced using the semi-analytical approach described in DR2.  
269 A: Growth rate values obtained for given values of  $\lambda/H$  for 0, 1, 2 and 3 weak layers. For each  
270 case, the characteristic wavelength value corresponds to the highest value of growth rate (e.g.,  
271 white star for the case with 3 weak layers). Insets show results of numerical simulations after 5.5  
272 Myrs, which develop folds with a spacing that is in excellent agreement with the predicted  
273 characteristic wavelength. A single basalt décollement layer results in small folding growth rates  
274 and in thrust-dominated deformation. Addition of one or more weak layers to the brittle  
275 sedimentary cover results increases the growth rate significantly and leads to folding-dominated  
276 deformation. The ZFB brown area corresponds to the  $\lambda/H$  ratio of the Zagros Fold Belt. B:  
277 diagrams of characteristic wavelength (left) and corresponding growth rate (right) versus  
278 viscosity of the weak layers and friction angle of the crust. Thick white lines show the  
279 constraints for Zagros Fold Belt (average  $\pm$  1 standard deviation). As in the Zagros Fold Belt  
280 salt viscosity is constrained independently, the best-fit friction angle for the crust is  $5\pm 5^\circ$ . The  
281 white star corresponds to the simulation of figure 3.  
282 <sup>1</sup>GSA Data Repository item 2011xxx, xxxxxxxx, is available online at  
283 [www.geosociety.org/pubs/ft2011.htm](http://www.geosociety.org/pubs/ft2011.htm), or on request from [editing@geosociety.org](mailto:editing@geosociety.org) or Documents  
284 Secretary, GSA, P.O. Box 9140, Boulder, CO 80301, USA.

**A**

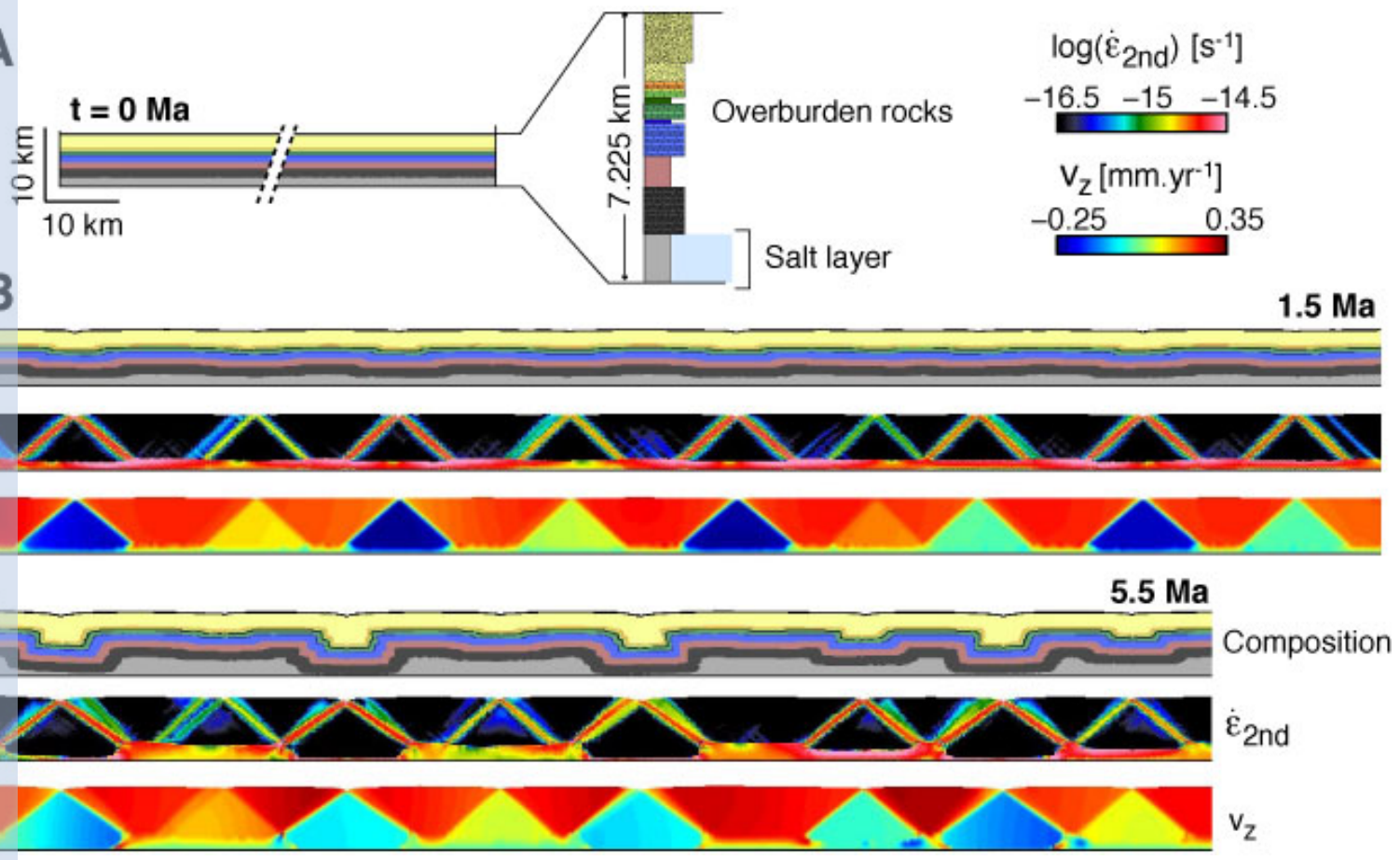


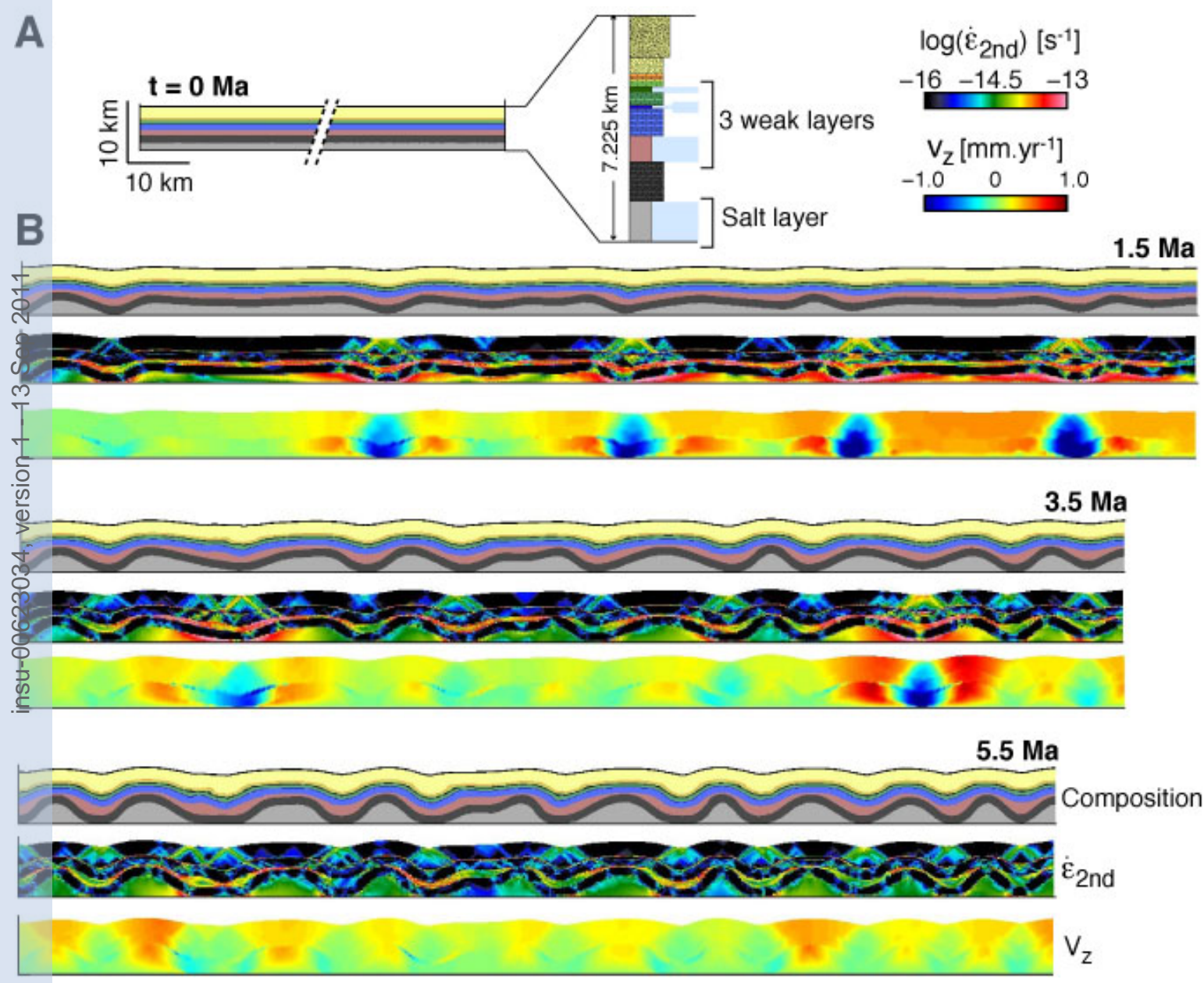
**C**

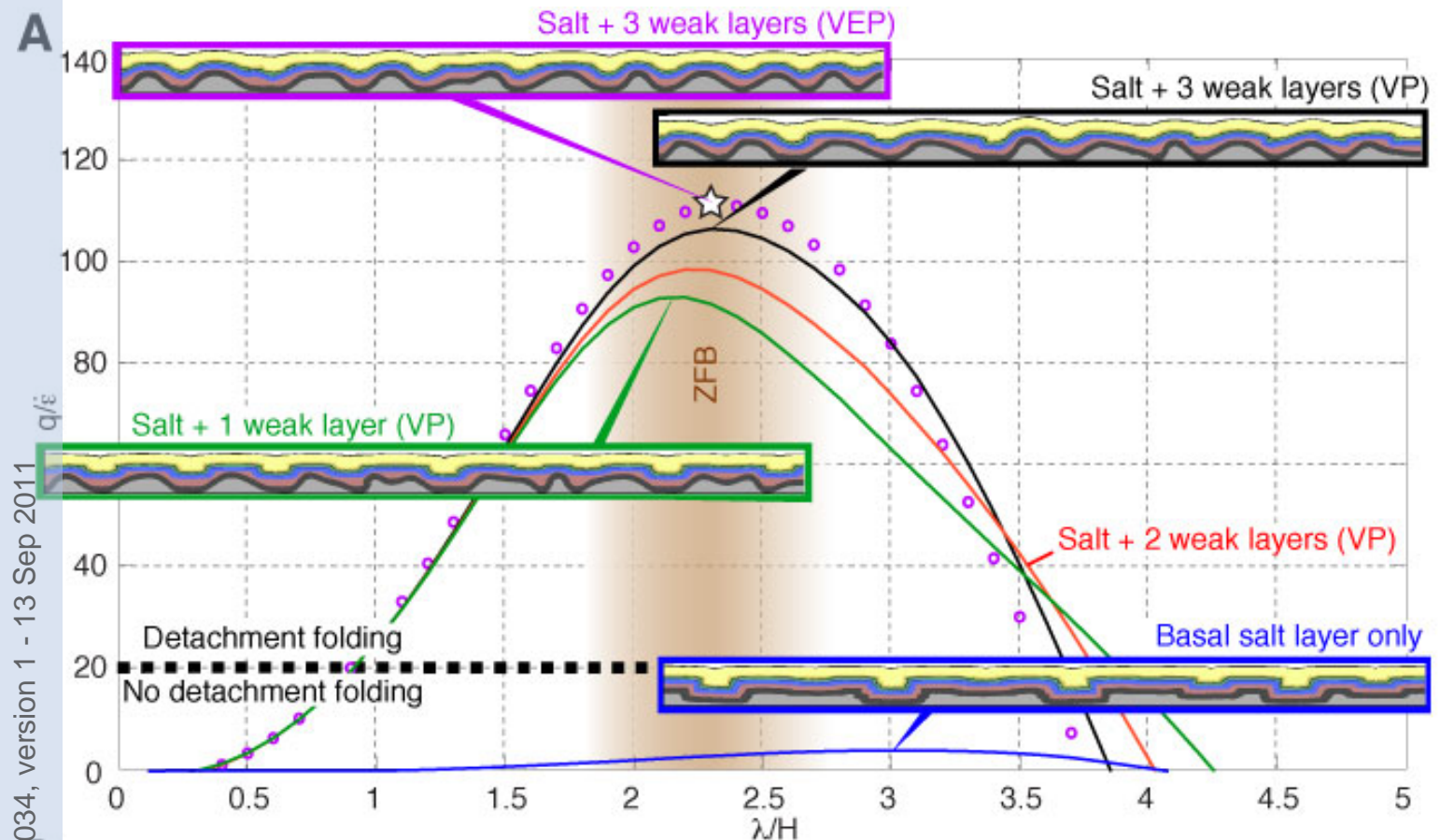


insu-00623034, version 1, 13 Sep 2011

**A**  
**B**







insu-00660034, version 1 - 13 Sep 2011

